

AD A 030875

AFML-TR-76-120

INHIBITION OF CRACK PROPAGATION OF HIGH STRENGTH STEELS THROUGH SINGLE AND MULTIFUNCTIONAL INHIBITORS

*METALS BEHAVIOR BRANCH
METALS AND CERAMICS DIVISION*

AUGUST 1976

TECHNICAL REPORT AFML-TR-76-120
FINAL REPORT FOR PERIOD JANUARY 1974 - NOVEMBER 1975

Approved for public release; distribution unlimited

DDC
RECEIVED
OCT 19 1976
RECEIVED
D

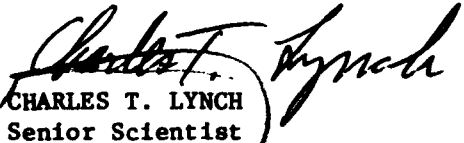
AIR FORCE MATERIALS LABORATORY
AIR FORCE WRIGHT AERONAUTICAL LABORATORIES
AIR FORCE SYSTEMS COMMAND
WRIGHT-PATTERSON AIR FORCE BASE, OHIO 45433

NOTICE


When Government drawings, specifications, or other data are used for any purpose other than in connection with a definitely related Government procurement operation, the United States Government thereby incurs no responsibility nor any obligation whatsoever; and the fact that the government may have formulated, furnished, or in any way supplied the said drawings, specifications, or other data, is not to be regarded by implication or otherwise as in any manner licensing the holder or any other person or corporation, or conveying any rights or permission to manufacture, use, or sell any patented invention that may in any way be related thereto.

This report has been reviewed by the Information Office (OI) and is releasable to the National Technical Information Service (NTIS). At NTIS, it will be available to the general public, including foreign nations.

This technical report has been reviewed and is approved for publication.


CHARLES T. LYNCH
Senior Scientist

FOR THE COMMANDER


VINCENT J. RUSSO
Chief, Metals Behavior Branch
Metals and Ceramics Division

Copies of this report should not be returned unless return is required by security considerations, contractual obligations, or notice on a specific document.

UNCLASSIFIED

SECURITY CLASSIFICATION OF THIS PAGE (When Data Entered)

REPORT DOCUMENTATION PAGE		READ INSTRUCTIONS BEFORE COMPLETING FORM
1. REPORT NUMBER AFML-TR-77-129	2. GOVT ACCESSION NO.	3. RECIPIENT'S CATALOG NUMBER
4. TITLE (and Subtitle) Inhibition of Crack Propagation of High Strength Steels through Single and Multifunctional Inhibitors.	5. DATES OF REPORT PERIOD COVERED Final report. 1 Jan 1974 - November 1975	
6. PERFORMING ORG. REPORT NUMBER		7. CONTRACT OR GRANT NUMBER(s)
8. AUTHOR(s) Charles T. Lynch, Kirit J. Bhansali Phillip A. Parrish		9. PROGRAM ELEMENT, PROJECT, TASK AREA & WORK UNIT NUMBERS 62162F 735106B2
10. CONTROLLING OFFICE NAME AND ADDRESS Air Force Materials Laboratory AFML/LLN Wright-Patterson Air Force Base, Ohio 45433		11. REPORT DATE August 1975
12. NUMBER OF PAGES 30		13. SECURITY CLASS. (of this report) UNCLASSIFIED
14. MONITORING AGENCY NAME & ADDRESS (if different from Controlling Office) 1237F		15. DECLASSIFICATION DOWNGRADING SCHEDULE
16. DISTRIBUTION STATEMENT (of this Report) Approved for public release; distribution unlimited. 16 AF-7351 17 735106		
17. DISTRIBUTION STATEMENT (of the abstract entered in Block 20, if different from Report)		
18. SUPPLEMENTARY NOTES		
19. KEY WORDS (Continue on reverse side if necessary and identify by block number) Corrosion Inhibitors High Strength Steels Hydrogen Embrittlement Inhibitors Oxidizing Inhibitors Crack Growth		
20. ABSTRACT (Continue on reverse side if necessary and identify by block number) Oxidizing inhibitors may be used to retard crack propagation for high strength low alloy steels. For D6AC the use of such inhibitors gives promise of being able to avoid hydrogen embrittlement. The critical stress intensity factor K_{Isc} apparently may also be manipulated by use of oxidizing inhibitors. Preliminary data on multifunctional inhibitors indicate that combinations of cathodic and anodic types is more effective than the common anodic inhibitors such as chromate. Hydrazine and the related nitrite ion are more effective inhibitors than chromate for steel in the presence of chlorides.		

DD FORM 1 JAN 73 1473 EDITION OF 1 NOV 65 IS OBSOLETE

UNCLASSIFIED

SECURITY CLASSIFICATION OF THIS PAGE (When Data Entered)

012320

FOREWORD

This report was prepared by the Metals Behavior Branch, Metals and Ceramics Division, Air Force Materials Laboratory, Air Force Wright Aeronautical Laboratories, Air Force Systems Command, Wright-Patterson Air Force Base, Ohio, 45433. It was initiated under Project 7351, "Metallic Materials for Air Force Weapon System Components", Task 735106, "Behavior of Metals", Inhouse Work Unit 735106B2, "Environmental Effects". The work was performed by Dr. Charles T. Lynch, Dr. Kirit J. Bhansali, a National Research Council Research Associate assigned to the Air Force Materials Laboratory from 1974 to 1976, and Dr. Phillip A. Parrish, who is currently with the Army Research Office, P.O. Box 12211, Research Triangle Park, NC, 27709. Dr. Parrish was formerly a Project Engineer at the AFML.

The report covers work conducted from January 1974 through November 1975. It was given in part at the Triservice Corrosion of Military Equipment Conference in October 1974. The report was submitted by the authors in June 1976.

The authors wish to express their thanks to Messrs. Linwood Golf and Barrett Blackwell for their help in obtaining the experimental results and to Mrs. Jean Gwinn and Mrs. Sally Gardner for typing the manuscript.

ACCESSION for	
NTIS	White Section <input checked="" type="checkbox"/>
DDC	Buff Section <input type="checkbox"/>
UNANNOUNCED	<input type="checkbox"/>
JUSTIFICATION.....	
BY.....	
DISTRIBUTION/AVAILABILITY CODES	
Dist.	Avail.
A	

D D C
 RECD
 OCT 19 1976
 RECD
 D

TABLE OF CONTENTS

SECTION	PAGE
I. INTRODUCTION	1
1. The Pressure Theory.	1
2. Lattice Decohesion Theory.	2
II. EXPERIMENTAL	2
1. Crevice Corrosion Characteristics of D6AC.	2
2. K_{ISCC} and Crack Growth Rate Studies.	2
3. Determination of pH within a Propagating Crack	3
4. Analysis for Localized Hydrogen.	3
III. RESULTS.	4
1. Chemical Composition of D6AC	4
2. Artificial Crevice Cell and Crack Tip pH Measurements	4
3. K_{ISCC} and Crack Growth Rate Studies.	4
4. Hydrogen Analysis of Localized Areas of Fracture Surfaces.	6
IV. DISCUSSION	6
V. SUMMARY AND CONCLUSIONS.	9
REFERENCES	29

LIST OF TABLES

TABLE		PAGE
1.	Composition of D6AC Steel.	10
2.	Potential-pH Data, D6AC in Artificial Crevice Cell	11
3.	Measured pH at Tip of Propagating Crack in D6AC.	12
4.	Inhibitors--General Considerations	13
5.	Inhibitors--Compounds.	14

LIST OF ILLUSTRATIONS

FIGURE		PAGE
1.	D6AC Compact Tension Specimen.	15
2.	Double Cantilever Displacement Clip Gage in Position on Frac- ture Toughness Specimen in Testing Grips	16
3.	Artificial Crevice Cell Results, pH 2.1 to 8.1	17
4.	Artificial Crevice Cell Results, 2% Hydrazine Addition to 0.1M NaCl Solution	18
5.	Crack Growth in Distilled Water.	19
6.	Crack Growth in Sodium Chloride and Sodium Bicarbonate at pH 8.5	20
7.	Crack Growth in Sodium Chloride, Sodium Bicarbonate, and Hydrazine.	21
8.	Crack Growth in Sodium Dichromate.	22
9.	Crack Growth in Distilled Water; Then Sodium Dichromate Added.	23
10.	Crack Growth in Sodium Chloride; Then Sodium Dichromate Added.	24
11.	Localized Hydrogen Analysis--D6AC Fractured in Distilled Water and Frozen in Liquid N ₂	25
12.	Localized Hydrogn Analysis, D6AC Fractured in Distilled Water Plus 2% Hydrazine and Frozen in Liquid N ₂	26
13.	Environmental Protection High Strength Steel	27
14.	Crack Growth in Distilled Water; Then Sodium Dichromate and Calgon Added	28

SECTION 1. INTRODUCTION

High strength alloys of steel are protected against general corrosion and corrosion reactions that lead to failure by stress corrosion cracking, hydrogen embrittlement, and corrosion fatigue, by an involved series of treatments. These typically will include shot peening, cadmium plating, and paint coatings consisting of inhibited primers and followed by a topcoat to protect over the primer coat. The inhibitor is important to this protective scheme, but routinely a chromate system is selected, and no other possibilities considered. In this paper, other inhibitors have been investigated for their ability to retard crack propagation from corrosion reactions in aqueous media.

There has been general disagreement in the literature concerning the mechanism by which aqueous environments induce failure of high strength steels at stress levels much less than their yield strengths. Two principal mechanisms have received the most support: (1) active path corrosion cracking^{1,2} and (2) hydrogen embrittlement.³ Active path corrosion (APC) theory holds that cracking occurs by anodic dissolution following a pre-existing susceptible path in the matrix. The susceptible path may be the result of grain boundary precipitation, or plastic deformation and/or precipitation ahead of the crack tip. Accordingly by this theory, crack growth is controlled by anodic dissolution.

"Hydrogen embrittlement cracking" (HEC) theory contends that the factor which controls crack growth is the absorption of nascent hydrogen by the metal. The average hydrogen content necessary to embrittle high strength steel alloys is of the order of 1-2 ppm.⁴ Snoek relaxation peaks have been observed^{5,6} for hydrogen in b.c.c. iron, indicating that atomic hydrogen enters the iron lattice and occupies interstitial sites.

There are two different, basic theories for the mechanism of hydrogen embrittlement. These have been reviewed extensively since 1960.⁷⁻¹³

1. The Pressure Theory¹⁴⁻¹⁹

This theory states that the precipitation of hydrogen gas at defects such as inclusions causes microcracks and voids because of high internal pressure at these points. The applied stress necessary for crack growth, σ_F , is lowered by this internal gas pressure, P.

$$\sigma_F - P = \frac{\sqrt{2E\gamma_p}}{\pi C} \quad \text{where } (\sigma \ll \sigma_y)$$

Where 2C = crack length

E = elastic modulus

γ_p = plastic work necessary to initiate an unstable fracture at crack tip.

2. Lattice Decohesion Theory

An alternative mechanism for hydrogen embrittlement has been proposed by Troiano.⁷ It assumes that interstitial hydrogen atoms diffuse to regions of high triaxial stress ahead of a notch or stress raiser, and are trapped by the high dislocation densities at these locations. This local accumulation of hydrogen lowers the cohesive strength of the lattice.²⁰⁻²³ Failure occurs as a series of crack "bursts" resulting from a step-wise process involving (a) stress-induced diffusion of hydrogen causing significant segregation of hydrogen locally ahead of the advancing crack, (b) the influence of interstitial hydrogen in localized cracking which results in the microcrack connecting with the advancing crack front.

M. Pourbaix²⁴ presented evidence that conditions prevalent in pits and crevices are not the same as those in the bulk. Efird²⁵ has described an "artificial crevice cell" and discussed "crevice" conditions with respect to the experimental potential-pH diagram for 90-10 Cu-Ni alloy studied by Parrish.²⁶ Brown et al.²⁷ using indicators to check the pH at the tip of a frozen crack as the solution at the crack tip thawed, reported that for cracks growing in 7075 aluminum and 0.45 C steel specimens immersed in either distilled water or sodium chloride solution of pH = 6.5, the indicated crack tip pH was consistently 3.5 to 3.8. In subsequent investigations, they devised an experiment²⁸ to measure the pH and electrode potential at the edge of a propagating crack in AISI 4340, high strength martensitic steel, in 0.6M NaCl solution. For a wide variety of electrochemical conditions in the bulk cell, the crack tip conditions were virtually independent of the bulk pH and potential. In all cases, the electrochemical conditions at the crack tip were such that hydrogen would be evolved. Leckie et al.²⁹ reported hydrogen gas was evolved from a precracked AISI 4340 specimen in sodium chloride solution. Parrish et al.³⁰ also observed hydrogen evolution at the crack tip of a compact tension specimen of D6AC steel anodically polarized in a corrosion fatigue experiment.

SECTION II. EXPERIMENTAL

1. Crevice Corrosion Characteristics of D6AC

Crevice corrosion characteristics of D6AC in 0.1N NaCl solution were studied as a function of bulk solution pH in a stirred, aerated solution at a temperature of 25°C. The artificial crevice cell used was similar to that designed by Efird.²⁵ The crevice solution was separated from the bulk solution by a 4μ porosity, fritted-glass disc. The exposed area of the bulk specimen was 16 cm² and that of the crevice specimen was 1 cm². The pH and potential were measured in the crevice compartment. The details of the artificial crevice cell have been previously described.³¹

2. K_{Isc} and Crack Growth Rate Studies

Compact tension specimens of D6AC, as shown in Fig. 1, were used to determine the K_{Isc} and crack growth rates in various environments. The specimen geometry corresponded with ASTM requirements for plane strain conditions.

The specimens were stressed laterally to facilitate the immersion of the specimens into a cell containing the solution required for the test by a lateral stressing frame incorporated into a creep machine. The details of experimental arrangements are available elsewhere.³¹ The cracking length was measured by a double cantilever displacement clip gage and compliance curves. Figure 2 shows this gage in place on a typical specimen obtained for actual crack length, a , as a function of crack opening displacement measured from the clip gage output at various loads. Using the crack length, a , and the load, P , data, the stress intensity factor, K_I , and the crack growth rate da/dt were determined by computer according to the following equation:³¹

$$K_I = \frac{P}{BW^{3/2}} \left[29.6 \left(\frac{a}{W} \right)^{1/2} - 185.5 \left(\frac{a}{W} \right)^{3/2} + 655.7 \left(\frac{a}{W} \right)^{5/2} - 1017.0 \left(\frac{a}{W} \right)^{7/2} + 638.9 \left(\frac{a}{W} \right)^{9/2} \right]$$

where B and W are the dimensions indicated in Fig. 1. B and W are selected to satisfy plane-strain conditions such that B and $a > 2.5(K_{Ic}/T_{ys})^2$ where K_{Ic} is the fracture toughness and T_{ys} is the tensile yield strength.

The determination of K_{Isc} and da/dt for D6AC in this manner gives a quantitative means of measuring the susceptibility to stress corrosion cracking of the alloy in various aqueous environments, and can indicate the effectiveness of the chemical addition to the bulk solution in preventing or retarding crack propagation at loads less than the critical stress intensity K_{Ic} .

3. Determination of pH Within a Propagating Crack

It is possible to measure the pH at the tip of the propagating crack by employing the indicator method of Brown et al.²⁷ The pH at the tip of a propagating crack was measured by removing the test cell from the load frame and immediately immersing the assembly in liquid nitrogen. This froze the solution contained at the crack tip. The specimen was then broken in air by overloading. Strips of indicator paper, applied to the frozen fracture surface gave the determination of pH at the crack tip as the solution melted.

4. Analysis for Localized Hydrogen

The localized concentrations of hydrogen as a function of position across the fracture surface on specimens which failed in noninhibited and in inhibited solution were compared by utilization of the unique ultrasensitive hydrogen membrane detector system which was developed by Das.³² The instrument works on the principle of selective permeation of hydrogen through a palladium alloy membrane at elevated temperatures from an argon carrier gas stream. Hydrogen is extracted by induction heating of the sample to its melting point or by selective melting using a point heat source such as an electric arc or laser beam. The hydrogen is quantitatively determined at less than 1 ppm by the increase in pressure

on the ultrahigh vacuum pumping station on the other side of the membrane.

SECTION III. RESULTS

1. The chemical composition of D6AC is given in Table 1.

2. Artificial Crevice Cell and Crack Tip pH Measurements

The results of artificial crevice cell (Table 2), and pH measurements within propagating cracks (Table 3) were in agreement with the previously reported studies by Brown et al.²⁷ In Fig. 3, the data points shown as black squares with initial bulk pH values ranging from 2 to 8 were superimposed on the experimental pH-potential diagram for D6AC in 0.1M Cl⁻ solution.³³ For each condition of initial bulk pH and potential, the steady-state crevice conditions were favorable for hydrogen evolution and subsequent embrittlement of the alloy. The black circular data points numbered 3-9 inclusive in Fig. 8 represent bulk sample electrode potentials and pH's of the bulk solution. No hydrogen evolution would occur at these potentials and pH's. Black circles numbered 1 and 2 are below the potential of the equilibrium hydrogen electrode and are in the domain of hydrogen evolution. The black square data points numbered 1-9 inclusive are the electrode potentials and resulting pH's in the occluded cell for the corresponding "crevice" specimens. It is seen that the crevice was acidified (pH lowered) and the potential shifted to more negative values, with the steady-state conditions in all cases shifted below the hydrogen evolution line.

The pH measurements at the tips of actual propagating cracks in D6AC, exposed to solutions of pH = 5.9 (distilled water) and 8.5 (0.1M NaCl + 0.1M NaHCO₃), obtained by Brown's indicator method, agreed with the artificial crevice results. The crack tip was acidified such that the pH values measured were 4.8 and 4.5, respectively.

In solutions containing oxidizing inhibitors, no significant shift of crevice condition occurred (i.e., no acidification). The measured electrode potentials were much higher (more noble than) the electrode potential of the equilibrium hydrogen electrode.

The pH measurements at the tip of a propagating crack exposed to solutions containing the oxidizing inhibitor, hydrazine, illustrate this behavior and are shown in Fig. 4.

3. K_{Isc} and Crack Growth Rate Studies

K_{Isc} and crack growth rate tests for D6AC were carried out in distilled water and solutions containing single or combinations of oxidizing inhibitors and with or without added sodium chloride.

a. Crack growth in distilled water.

The crack growth rate in distilled water as a function of stress intensity is shown in Figure 5. The K_{Isc} was approximately 29 ksi $\sqrt{\text{inch}}$

with a crack growth rate between 3×10^{-6} and 5×10^{-5} in/min. The K_{Ic} from this curve is at about 110 ksi $\sqrt{\text{inch}}$ and fell in the range of 105-120 ksi $\sqrt{\text{inch}}$ in these experiments.

b. Crack growth in 0.1M NaCl and 0.1M NaHCO₃.

The NaHCO₃ solution at pH 8.5 is not particularly effective in the presence of NaCl as seen in Fig. 6. The K_{Isc} was shifted perhaps slightly to higher values, and the crack growth rate remained very constant at 5×10^{-5} in/min.

c. Crack growth in 0.1M NaCl, 0.1M NaHCO₃, and 2% hydrazine.

The addition of hydrazine to the previous type solution raised the K_{Isc} to 60 ksi $\sqrt{\text{inch}}$ and lowered the crack growth rate to 1×10^{-5} to 9×10^{-5} in/min. as given in Fig. 7.

d. Crack growth in 0.1M Na₂Cr₂O₇.

Figure 8 indicates that Na Cr₂O₇ acts to increase K_{Isc} to 77 ksi $\sqrt{\text{inch}}$ and lower the crack growth rate to 8×10^{-6} in/min. Lowering the concentration of Na₂Cr₂O₇ to 0.005 M decreased the K_{Isc} and increased the crack growth rates to values comparable to those obtained in distilled water. Thus in chloride-free solutions chromates can be beneficial if present in sufficiently large concentrations.

An experiment was devised to test the ability of chromates to arrest a propagating crack in D6AC. Crack growth was initiated in chloride-free distilled water and allowed to reach steady-state crack growth (region II). Then, by removing some of the water and replacing it with Na₂Cr₂O₇ so that the solution finally consisted of 0.1M Na₂Cr₂O₇, the effect of inhibitor addition on crack growth was seen. As shown in Fig. 9, the crack propagation halted immediately after the Na₂Cr₂O₇ was added. After a waiting period of 48 hours (during which time the crack growth was arrested), the specimen was incrementally loaded and the crack started to grow once again at $K_I = 77$ ksi $\sqrt{\text{inch}}$, identical to the value for K_{Isc} in 0.1M Na₂Cr₂O₇ solution (compare with Fig. 8). The crack growth rates at this point were also similar.

e. Crack growth in 0.1M NaCl + 0.1M Na₂Cr₂O₇.

In the presence of 0.1M NaCl, the effectiveness of 0.1M Na₂Cr₂O₇ for crack prevention was diminished. The K_{Isc} was reduced to 50 ksi $\sqrt{\text{inch}}$ and the crack growth in region II increased to 3×10^{-5} in/min. Again in Fig. 10, the results are seen for a crack allowed to grow in distilled water containing NaCl this time, and then the Na₂Cr₂O₇ added. The Na₂Cr₂O₇ is not very effective in the presence of NaCl, with the crack growth rates comparable to those in water containing no inhibiting agent.

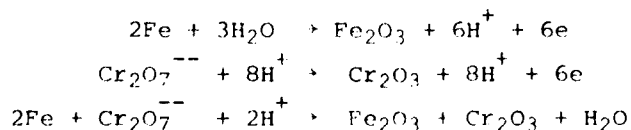
4. Hydrogen Analysis of Localized Areas of Fracture Surfaces

The D6AC compact tension specimens were fractured in distilled water and buffered solutions of 0.1M NaCl with and without inhibitor additions. Figures 11 and 12 show the results of local hydrogen analysis from tests conducted in distilled water and in hydrazine-inhibited distilled water, respectively. Samples were stored at liquid nitrogen temperature until hydrogen analysis could be made. Referring to Fig. 11, in the area of the fatigue-precrack zone which was exposed to distilled water environment for 8 hours before crack growth began, the hydrogen concentration was the highest (23.88 ppm). During region II crack growth, in which the crack propagated at a faster rate, the hydrogen concentration showed a considerable gradient. In the shear-lip area, which underwent fracture due to specimen overload, the hydrogen concentration was 8.25 ppm. At the end of fracture, and in the region of the machined notch (where no stress corrosion cracking occurred), the hydrogen level was 1.45 to 3.36 ppm which should be taken as the "baseline" hydrogen content of the specimen before exposure.

For the specimen fractured in distilled water containing 2% hydrazine, Fig. 12, the influence of hydrazine on the amount and distribution of hydrogen is shown dramatically. Nowhere on the specimen surface is the hydrogen content above the "baseline" range.

SECTION IV. DISCUSSION

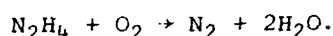
Without use of an oxidizing inhibitor, K_{Isc} values and cracking rates for D6AC (in distilled water) in region II were about 29 ksi $\sqrt{\text{inch}}$ and $4-7 \times 10^{-5}$ in/min. respectively. From the artificial crevice cell (confirmed by the indicator method of Brown et al.³⁰), it is clear that the pH and potential at the crack tip shifts to conditions favorable for hydrogen evolution. By the localized hydrogen analyses on the fracture surfaces, the cracking observed was associated with the presence of hydrogen and can reasonably be termed hydrogen embrittlement. However, when an oxidizing inhibitor such as N_2H_4 was added to the solution, K_{Isc} increased and crack growth rate decreased to about 60 ksi $\sqrt{\text{inch}}$ and 8×10^{-6} in/min. respectively. In this case, the pH and potential at the crack tip remained almost the same as in the bulk solutions and were therefore, unfavorable for hydrogen evolution. The localized hydrogen results tend to confirm the absence of hydrogen enrichment in the presence of oxidizing inhibitors. Sodium dichromate was an effective inhibitor in chloride free solutions but not in the presence of chlorides. The strong oxidizing capability of $Na_2Cr_2O_7$ oxidizes the D6AC surface to Fe_2O_3 as follows in the absence of chlorides:³¹



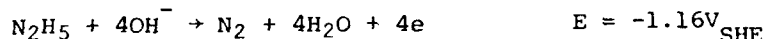
Both Fe_2O_3 and Cr_2O_3 film can protect the steel from corrosion and drive the corrosion potential into the passive region (above the hydrogen

evolution line). The chromium oxides are effective in blocking pores and other discontinuities in the Fe_2O_3 passive film, thus enhancing the passivating nature of the oxide film on the metal surface. However, the passivity of iron cannot be easily maintained in the presence of chloride ion in the solution. Chloride ion apparently attacks the passive film, at the crack opening up the crack tip region to rapid anodic dissolution and possibly lowering the electrode potential, below hydrogen evolution line at the low pH encountered, thereby causing hydrogen embrittlement.

Hydrazine is a well known inhibitor for corrosion of iron and steel, and is normally considered to be an oxygen scavenger³⁴⁻³⁵, i.e.,

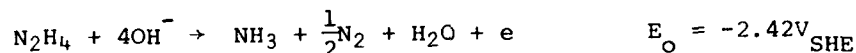


However, according to Evans,³⁶ hydrazine does not necessarily remove oxygen. He suggested the anodic reaction of hydrazine as

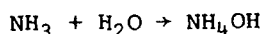


which is balanced by the cathodic reduction of O_2 . During experiments using the crevice corrosion cell, nitrogen gas, nitrite ion, and the odor of NH_3 were observed in the crevice compartment.

Jolly³⁷ reported formation of ammonia and nitrogen gas from hydrazine, i.e.

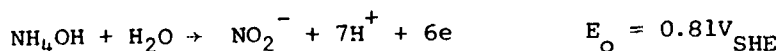
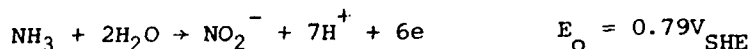


The ammonia is hydrated subsequently to ammonium hydroxide, i.e.,

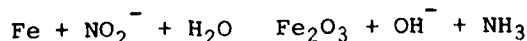


$$\log \frac{\text{PNH}_3}{(\text{NH}_4\text{OH})} = -1.75$$

The ammonia and ammonium hydroxide may be oxidized to nitrite ion^{38,39} by anodic polarization as follows:

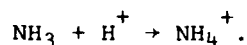
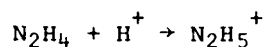


Thus, hydrazine also seems capable of inhibiting corrosion of iron in the range of electrode potential in which nitrite ion is stable since nitrite ion is a strong oxidizer, i.e.



When Cl^- ion exists in the solution, it attacks the passive film at the crack apex to induce low pH by the hydrolysis of metal ions. However,

hydrazine and its product, NH_3 , consume H^+ ion, i.e.,



These reactions are believed to prevent the pH and potential from falling below the hydrogen evolution line thereby preventing the cracking from hydrogen embrittlement. Therefore, any cracking under these conditions is attributed to stress-assisted anodic dissolution and/or active path corrosion. Artificial crevice cell experiments³¹ have confirmed that in the presence of $\text{Na}_2\text{Cr}_2\text{O}_7$, the crevice potential and pH remain well above the hydrogen line, similar to bulk measurements, but shift below the line in the presence of chloride, comparing unfavorably with the results for hydrazine previously shown in Fig. 4.

The results suggest the direct use of nitrite containing compounds for inhibiting action instead of hydrazine. Preliminary experiments with sodium nitrite indicate it is as effective, and perhaps more effective as hydrazine in lowering the crack growth rates in D6AC steel.

The major protective treatments for high strength steels are indicated schematically in Fig. 13. Of these, the function of the inhibitor systems is generally found in the primer coat. There are a number of considerations for the selection of suitable inhibitors. Foremost is the need for their compatibility with the epoxy or other primer paint, and the ability to inhibit or prevent both general corrosion and localized corrosion (by stress corrosion cracking, hydrogen embrittlement, or corrosion-fatigue). There are several considerations in the selection of suitable inhibitors. The protective coatings, themselves, in the as-applied state can be quite effective, providing that holidays in the coatings are minimized. The classic inhibitor with little variation is zinc chromate. Recently, some more soluble chromates have been examined to provide increased mobility in the inhibitor function. As coatings are damaged, eroded, fatigued, and otherwise failed in service, it is necessary to have a mobile inhibitor protective system in the inhibitor containing layer. Some general considerations for inhibitors are given in Table 4. The classic zinc chromate inhibitor serves as a basically single function anodic inhibitor with a limited solubility range. Chromates are toxic to human beings in the concentrations necessary to be effective for high strength steels. In the presence of chlorides, chromates are not effective in preventing hydrogen embrittlement. As seen in these results, there are other inhibitors which are more effective, especially in the presence of chloride ions.

This report has been concerned primarily with the action of anodic inhibitors and buffering agents. Another important class of inhibitors are those that act as cathodic inhibitors. They are generally not as effective as anodic inhibitors but can be very effective in combination with the anodic inhibitors. In fact, commercial inhibitors are often combinations of several classes of inhibitor compounds which are more

effective in combination than used separately.⁴⁰ Examples of such formulations are found in cooling towers, automobile radiators, etc. Some of these compound formulations are given in Table 5. As a follow on to this work, several combination formulations are being studied such as the borax-nitrite and polyphosphate (Calgon)-chromate systems. Results from crack growth measurements on D6AC steel in distilled water followed by the addition of chromate and a commercial polyphosphate (Calgon) are shown in Fig. 14. The crack growth rate in chromate is shown to compare with the addition of the polyphosphate which is seen to raise the K_{ISCC} from 77 to 82 ksi $\sqrt{\text{inch}}$ and lower the crack growth rate by about one-half an order of magnitude from 8×10^{-6} to 1×10^{-5} in/min. down to $3-5 \times 10^{-6}$ in/min. The results are sufficiently promising to direct further work in the direction of multifunctional inhibitor systems.

SECTION V. SUMMARY AND CONCLUSIONS

Oxidizing inhibitors can be utilized to retard crack growth in high strength, low alloy martensitic steels in aqueous solutions. Artificial crevice cell and crack tip pH measurements have shown that conditions favorable for hydrogen embrittlement of the steel exist in propagating cracks. Localized hydrogen measurements of the fracture surfaces of D6AC specimens which failed under tensile load in aqueous solution show that hydrogen was absorbed into the steel in the vicinity of the crack tip.

Hydrazine was effective in reducing the crack growth rate by one order of magnitude for D6AC in aqueous solution. A 2% addition of hydrazine to solution increased K_{ISCC} from 29 to 60 ksi $\sqrt{\text{inch}}$, in both 0.1 M NaCl and nil chloride solutions. Inhibition of crack growth by hydrazine was accompanied and related to the formation of nitride, NO_2^- , which in aqueous solution changed the crack tip conditions of pH and potential so that no hydrogen evolution occurred within the crack, and the passive $\gamma\text{-Fe}_2\text{O}_3$ film formed. Localized hydrogen analysis across the fracture surface of specimens which failed in these aqueous hydrazine solutions showed that no hydrogen was absorbed at the propagating crack tip. Thus, failure by hydrogen embrittlement was prevented.

Sodium dichromate was also effective in reducing crack growth rates in aqueous solution. For specimens exposed to 0.1 M $\text{Na}_2\text{Cr}_2\text{O}_7$ solution, the K_{ISCC} was raised from 29 to 77 ksi $\sqrt{\text{inch}}$ and the crack rate was reduced significantly. The $\alpha\text{-Fe}_2\text{O}_3$ and chromic oxide film formed was apparently not stable in the presence of chloride ions and the crack growth behavior not much better for chromate plus chloride than for D6AC steel in distilled water where K_{ISCC} was 29 ksi $\sqrt{\text{inch}}$ and the crack growth rate $3-5 \times 10^{-5}$ in/min. Preliminary results with multifunctional cathodic-anodic inhibitor formulations show promise of improved protection in the presence of chlorides.

TABLE 1
COMPOSITION OF D6AC STEEL

C = 0.45

Cr = 1.15

Ni = 0.55

Mo = 1.0

Mn = 0.8

Si = 0.25

V = 0.05

TABLE 2

POTENTIAL-pH DATA, D6AC IN ARTIFICIAL CREVICE CELL

Test No.	Solution No.	Bulk Potential (SCE)	Bulk pH	Crevice Potential (SCE)	Crevice pH
1	1	-0.536V	2.1	-0.597	2.7
2	1	-0.556	2.1	-0.603	2.9
3	2	-0.415	5.5	-0.525	4.9
4	2	-0.375	5.5	-0.515	4.7
5	2	-0.270	5.5	-0.510	4.3
6	3	-0.445	6.1	-0.560	3.7
7	3	-0.300	6.1	-0.505	4.0
8	4	-0.430	8.1	-0.560	5.0
9	4	-0.560	8.1	-0.578	4.9
10*	5	-0.142	9.9	-0.182	9.6
11*	5	-0.153	9.9	-0.175	9.5
12*	6	-0.100	4.0	+0.003	4.3
13*	6	-0.108	4.0	+0.012	4.4
14*	7	-0.050	4.3	-0.150	4.0
15*	7	-0.040	4.3	-0.138	4.0

Solution 1. 10 ml (1.0M HCl) + 90 ml (1.0M NaCl) + 900 ml Distilled H₂O

Solution 2. 100 ml (1.0M NaCl) + 10 ml (0.1M HCl) + 890 ml Distilled H₂O

Solution 3. 100 ml (1.0M NaCl) + 455 ml (0.1M NaOH) + 455 ml (0.1M KHC₈H₄O₄)

Solution 4. 100 ml (1.0M NaCl) + 900 ml Distilled H₂O

Solution 5. 0.1M NaCl + 2% N₂H₄.

Solution 6. 0.1M Na₂Cr₂O₇

Solution 7. 0.1M Na₂Cr₂O₇ + 0.1M NaCl

*Solution containing oxidizing inhibitor, see Table 3. Tests under freely corroding conditions.

TABLE 3

MEASURED pH AT TIP OF PROPAGATING CRACK IN D6AC

Environment	Crack Tip pH
1) Distilled H ₂ O (pH = 5.9)	4.8
2) 0.1M NaCl + 0.1M NaHCO ₃ (pH = 8.5)	4.5
3) 0.1M NaCl + 0.1M NaHCO ₃ + 2%N ₂ H ₄ (pH = 9.9)*	9.2
4) 0.005M Na ₂ Cr ₂ O ₇ (pH = 4.7)*	4.6
5) 0.1M Na ₂ Cr ₂ O ₇ (pH = 4.0)*	4.4
6) 0.1M NaCl + 0.1M Na ₂ Cr ₂ O ₇ (pH = 4.0)*	4.3
7) 0.1M NaCl + 0.1M NaHCO ₃ + 0.183M NaOH (pH = 9.9)	4.5
8) 0.1M NaCl + 0.1M NaHCO ₃ + 0.223M NaOH (pH = 10.5)	4.8

*Oxidizing inhibitor solutions

TABLE 4

INHIBITORS - GENERAL CONSIDERATIONS

MULTIFUNCTIONAL

Cathodic

Anodic

Chloride Absorbers

Buffers

SOLUBILITY RANGE

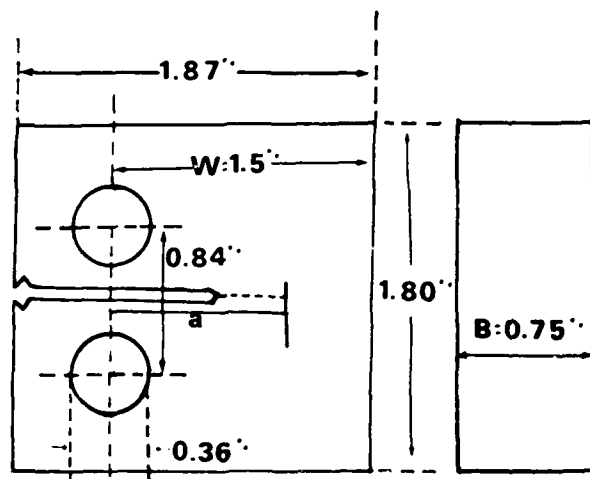
INFLUENCE HYDROGEN ENTRY RATES

TOXICITY

TABLE 5

INHIBITORS - COMPOUNDS

CATHODIC	Polyphosphate	Zinc	Silicate	
ANODIC	Orthophosphate	Chromate	Ferrocyanide	Nitrite
COMBINATIONS	Polyphosphate-Chromate			
	Polyphosphate-Ferrocyanide			
	Borax-Nitrite			
	Fluoride-Chromate			
	Benzoate-Nitrite			
	Silicate-Chromate			
FILM FORMERS	Emulsified or Soluble Oils			
	Octadecylamine			
	Long Chain Amines			
	Alcohols & Carboxylic Acids			



(Scale:1.5:1)

Compact Tension Specimen

Figure 1. D6AC Compact Tension Specimen.

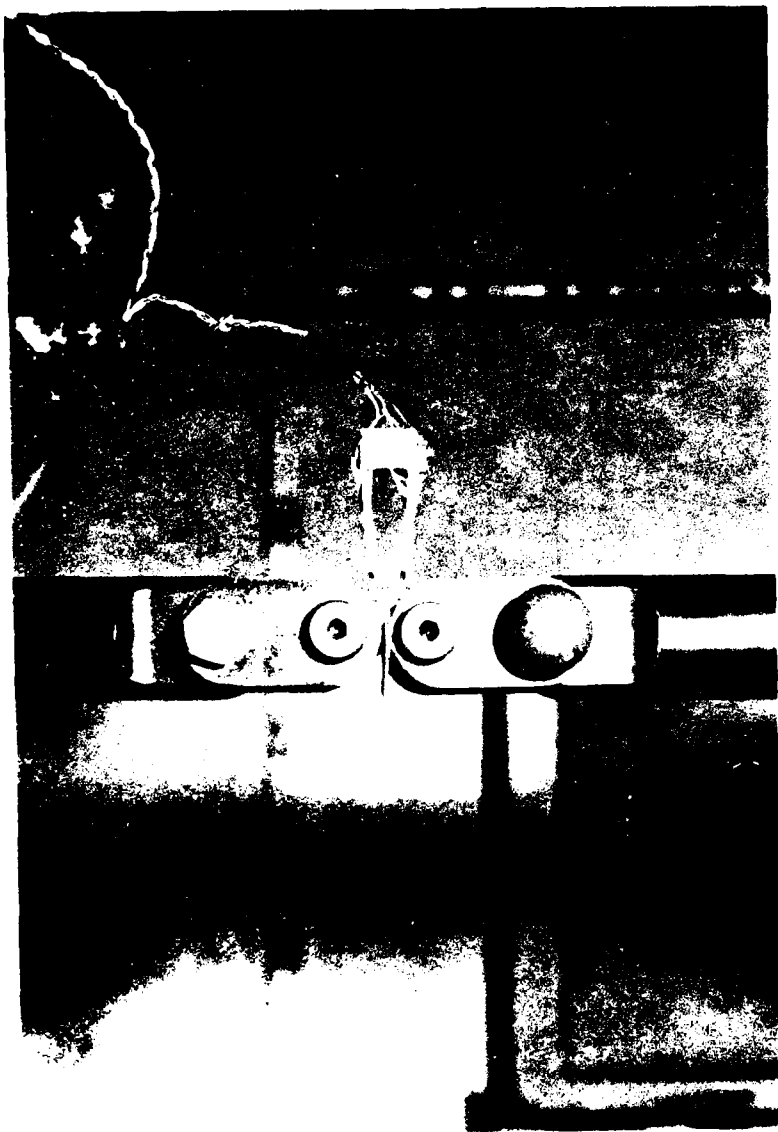
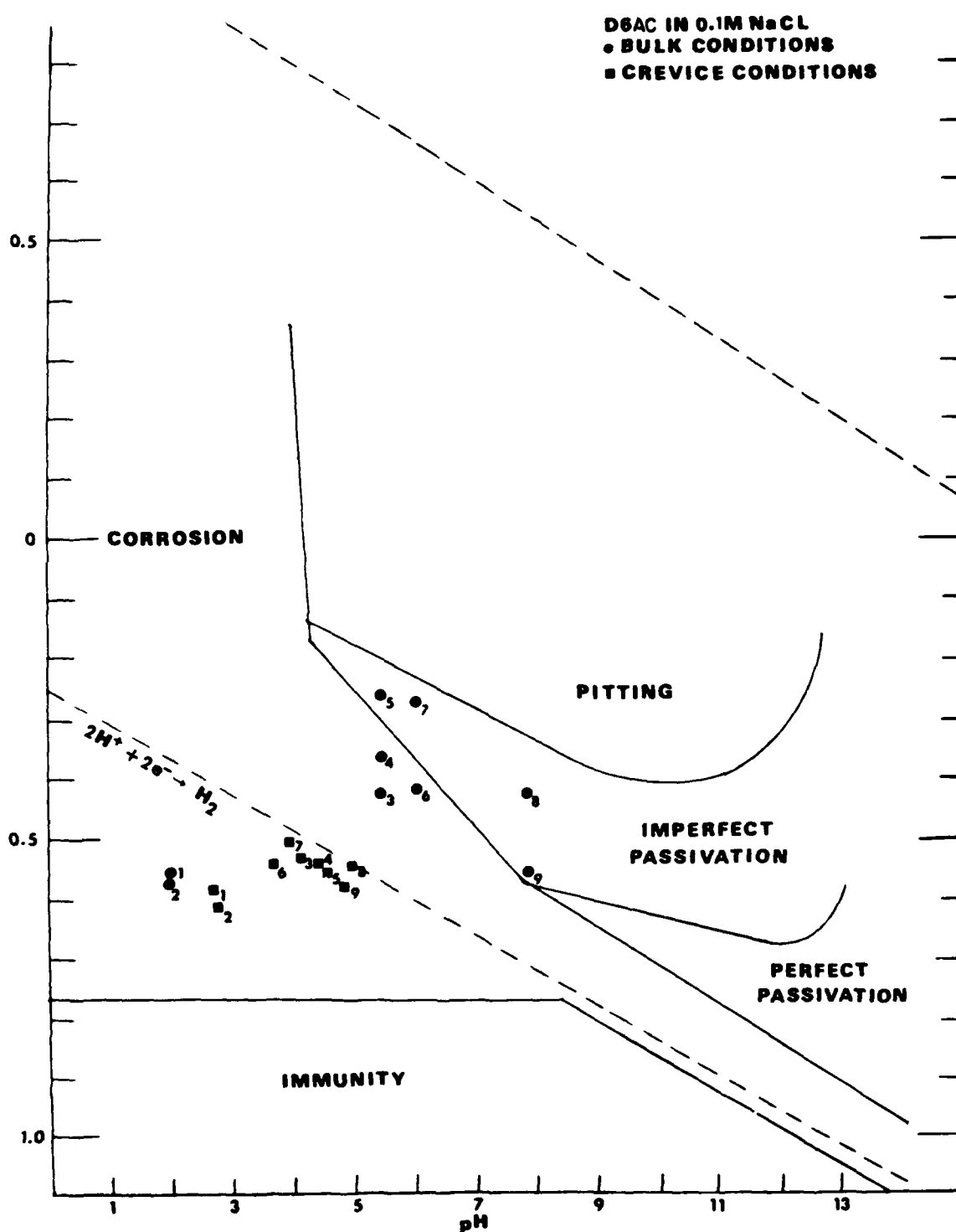


Figure 2. Double Cantilever Displacement Clip Gage in Position on Fracture Toughness Specimen in Testing Grips. Approx. 0.5X



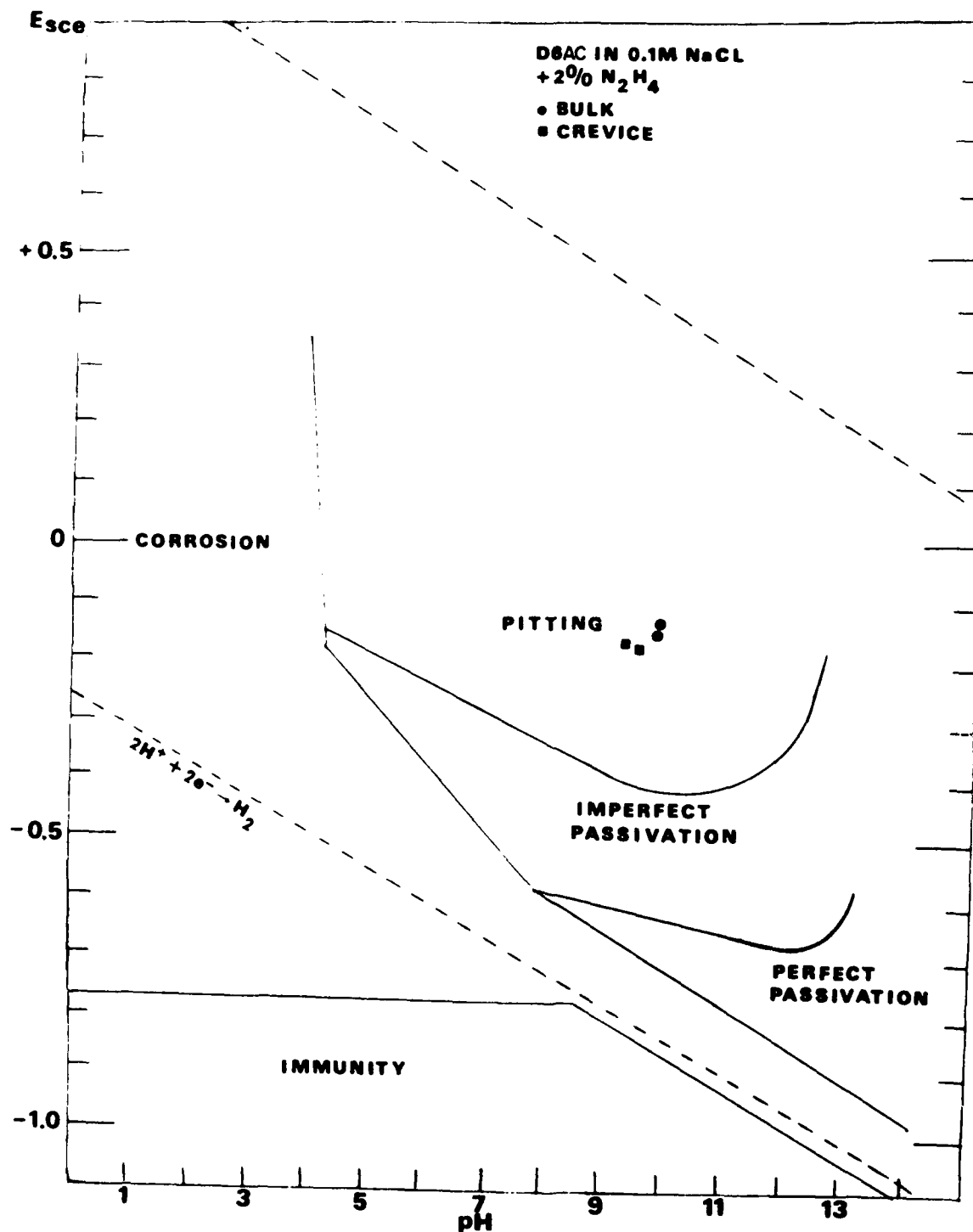
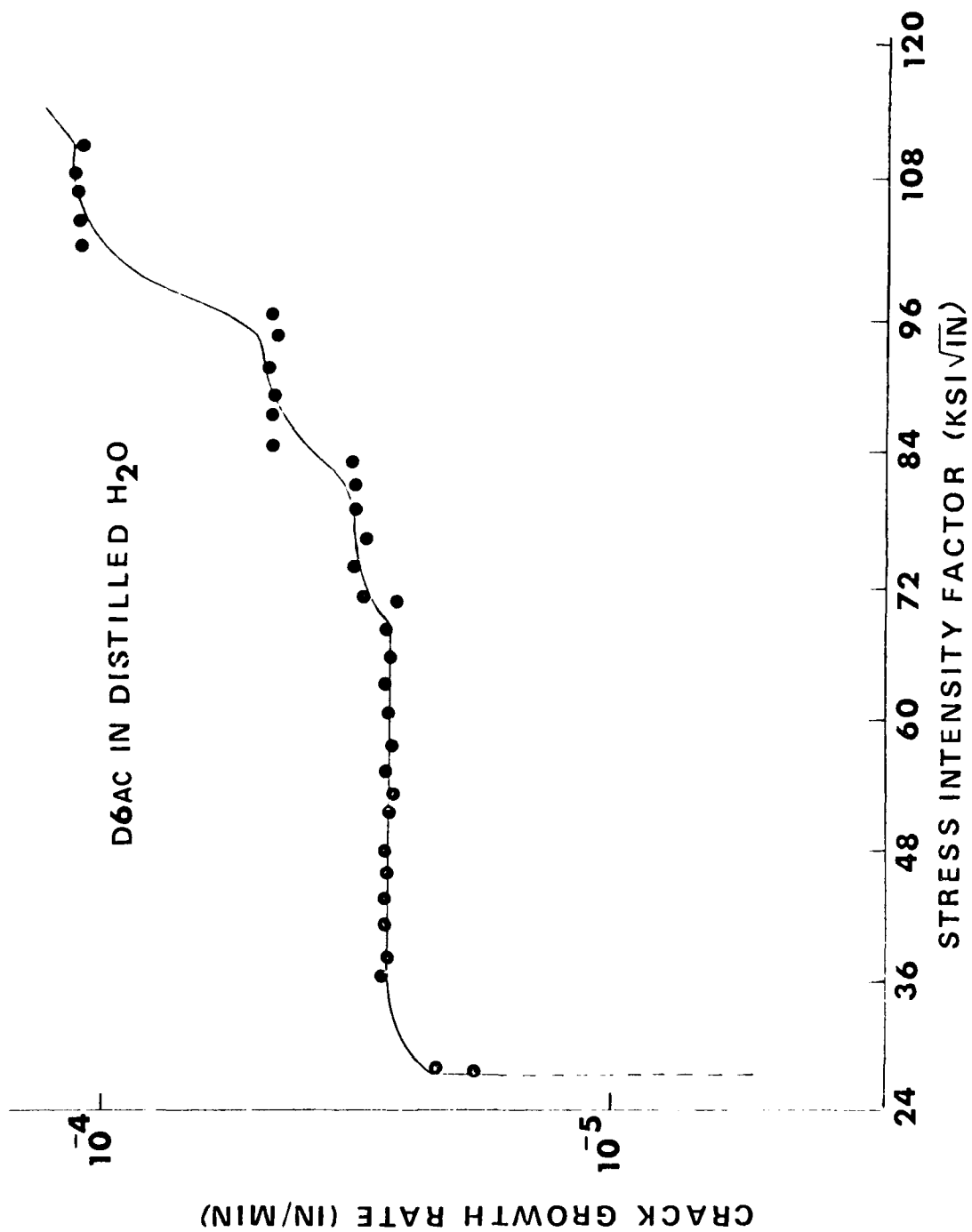


Figure 4. Artificial Crevice Cell Results, 2% Hydrazine Addition to 0.1M NaCl Solution.



D6AC IN 0.1M NaCl + 0.1M NaHCO₃

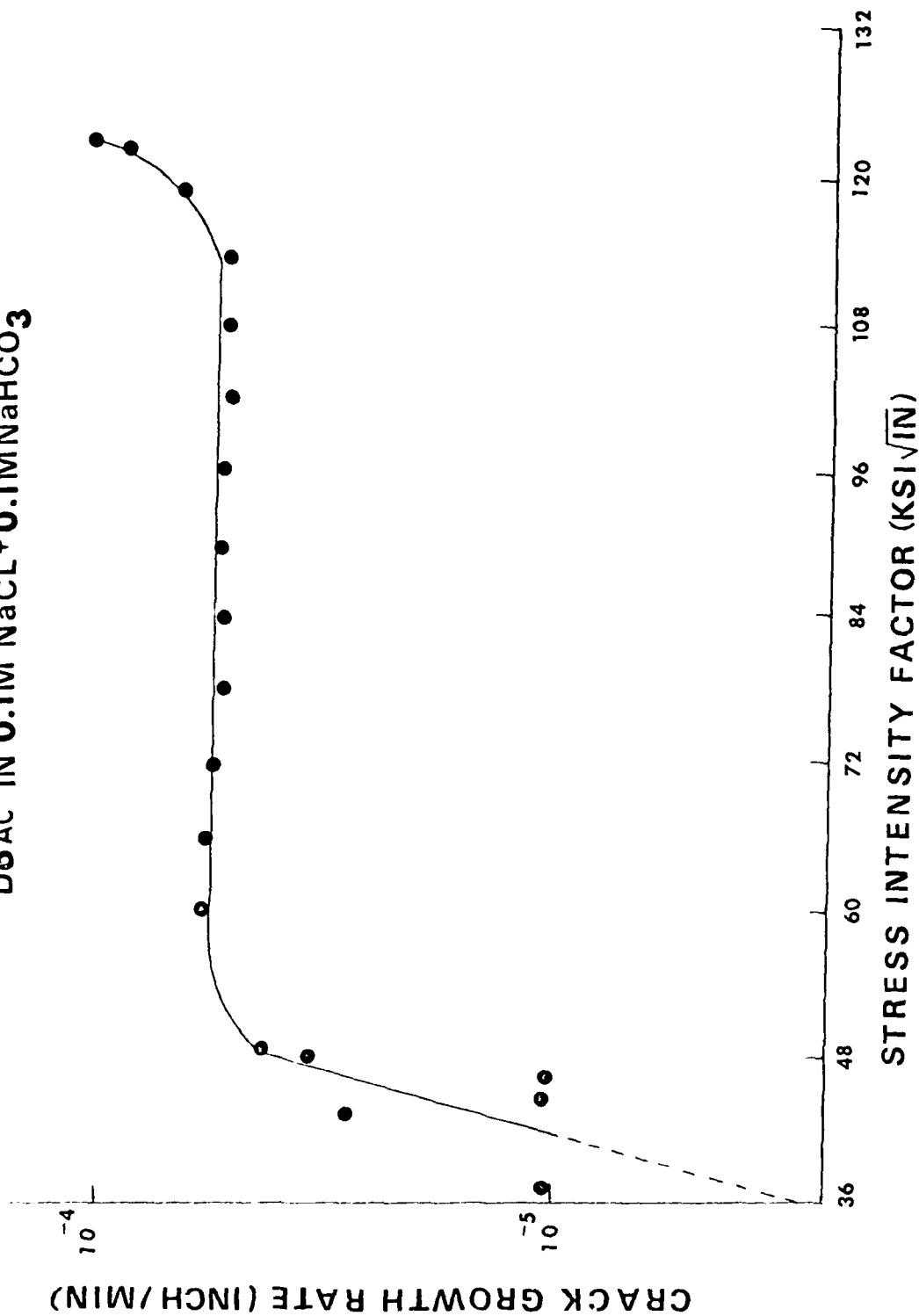


Figure 6. Crack Growth in Sodium Chloride and Sodium Bicarbonate at pH 8.5.

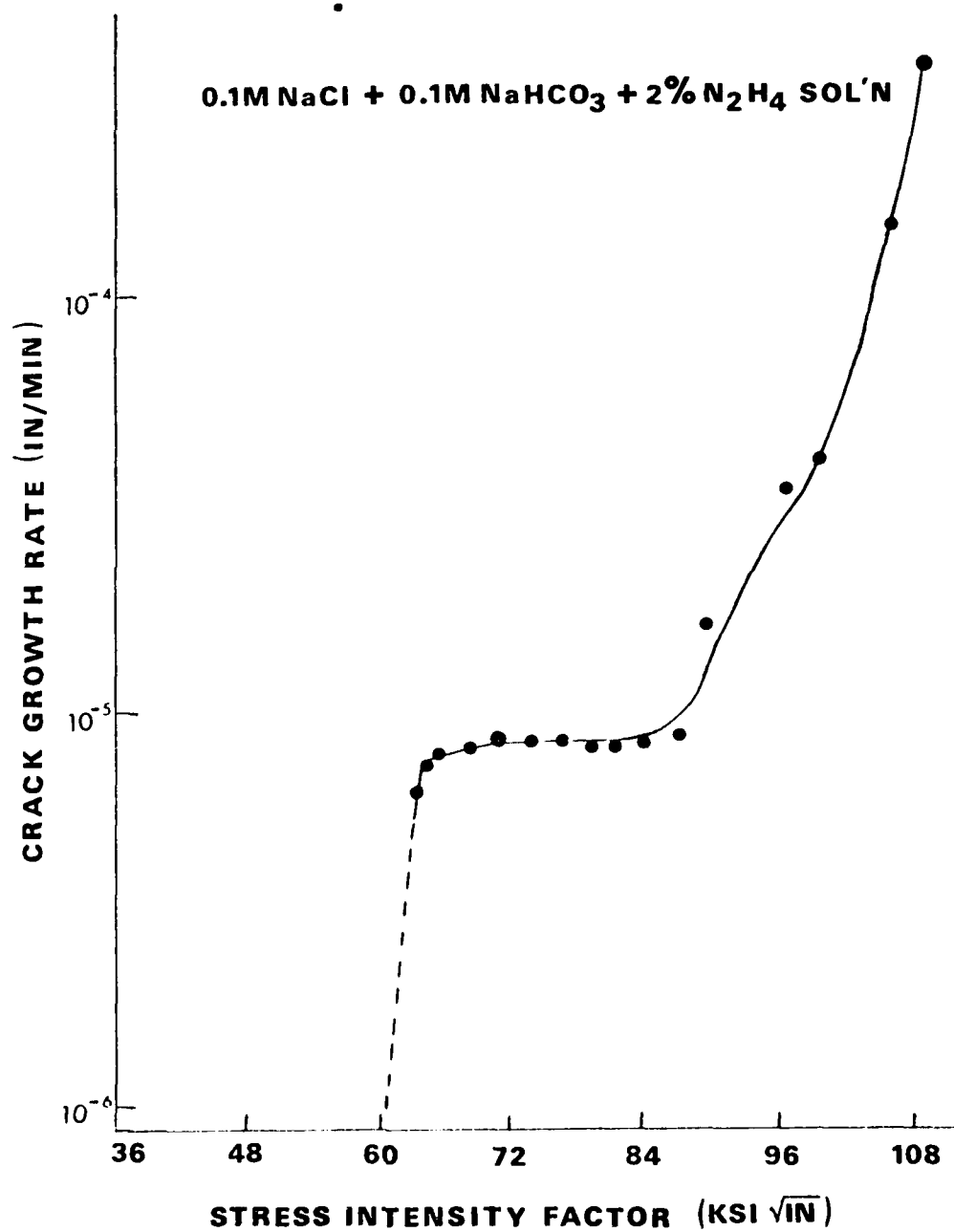


Figure 7. Crack Growth in Sodium Chloride, Sodium Bicarbonate, and Hydrazine.

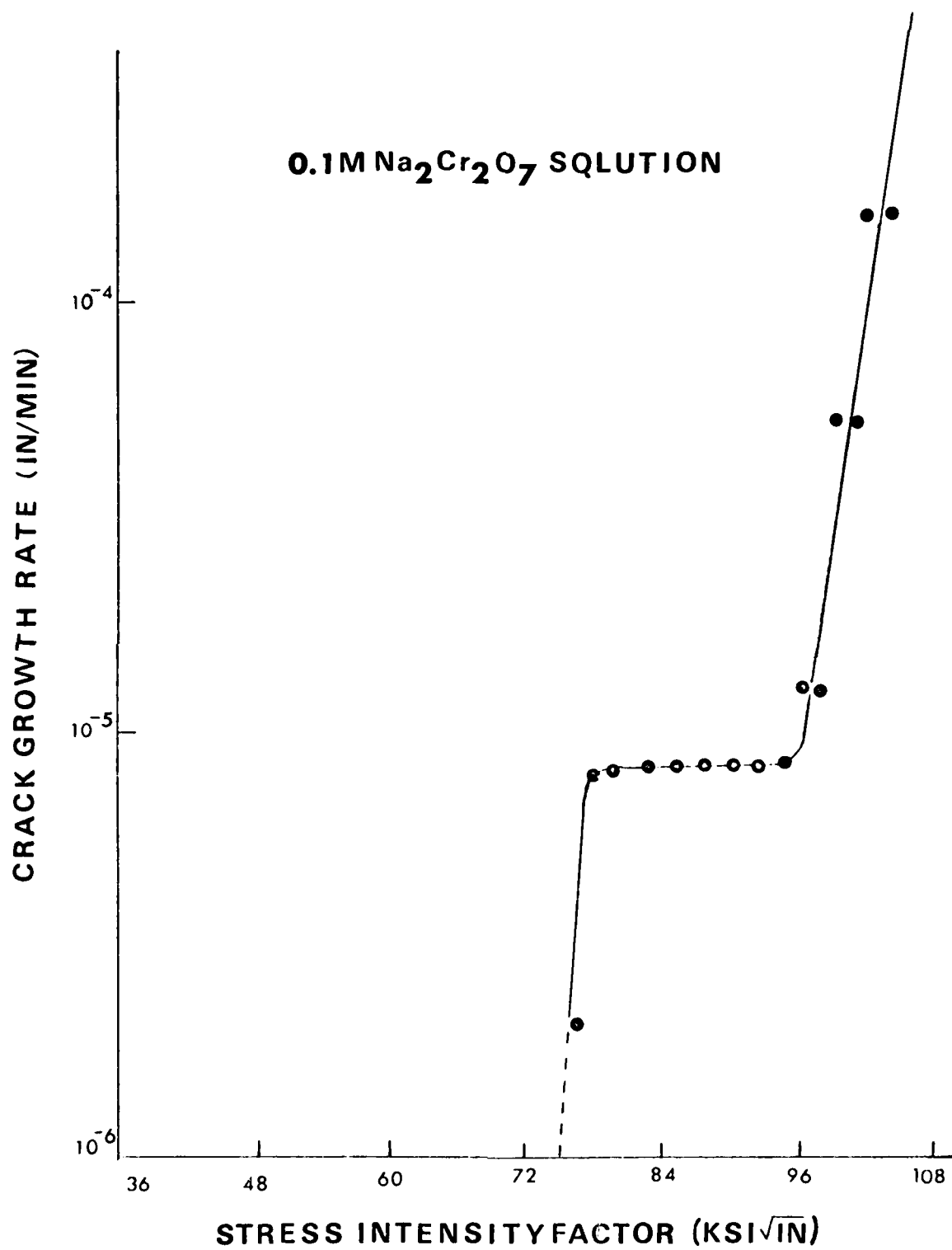


Figure 6. Crack Growth in Sodium Dichromate.

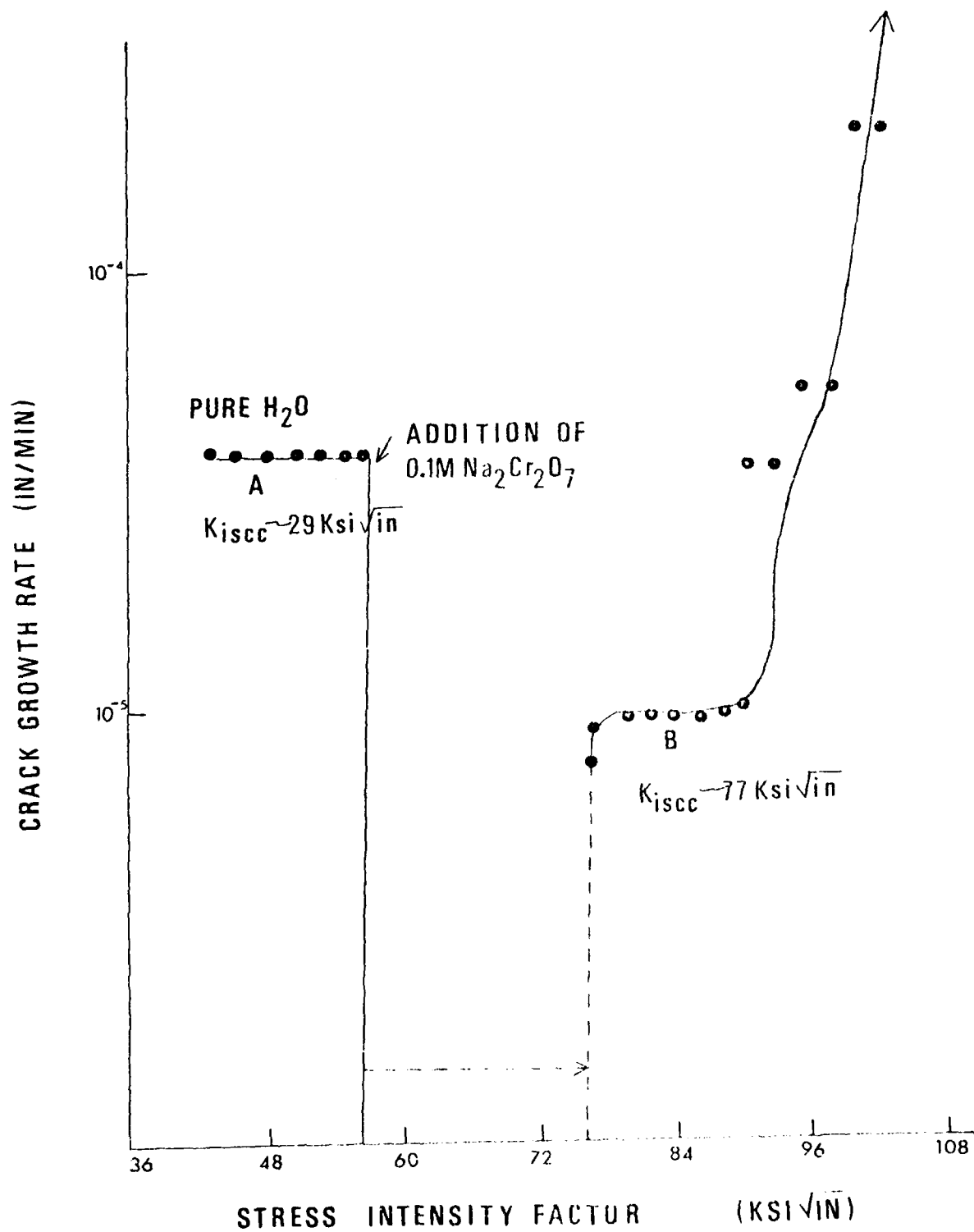


Figure 9. Crack Growth in Distilled Water; Then Sodium Dichromate Added.

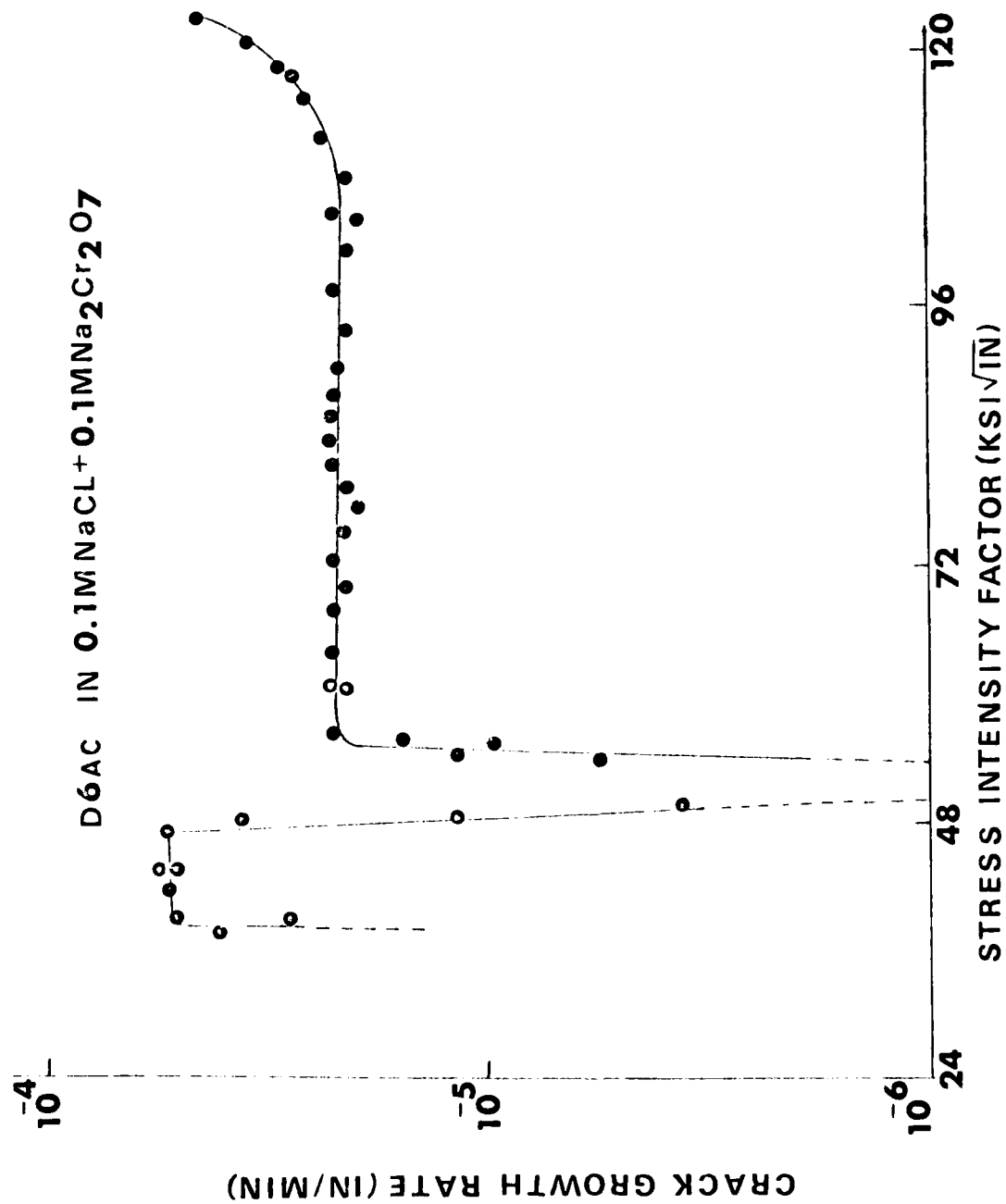


Figure 1. Crack growth in Sodium Chloride; Then sodium Dichromate added.

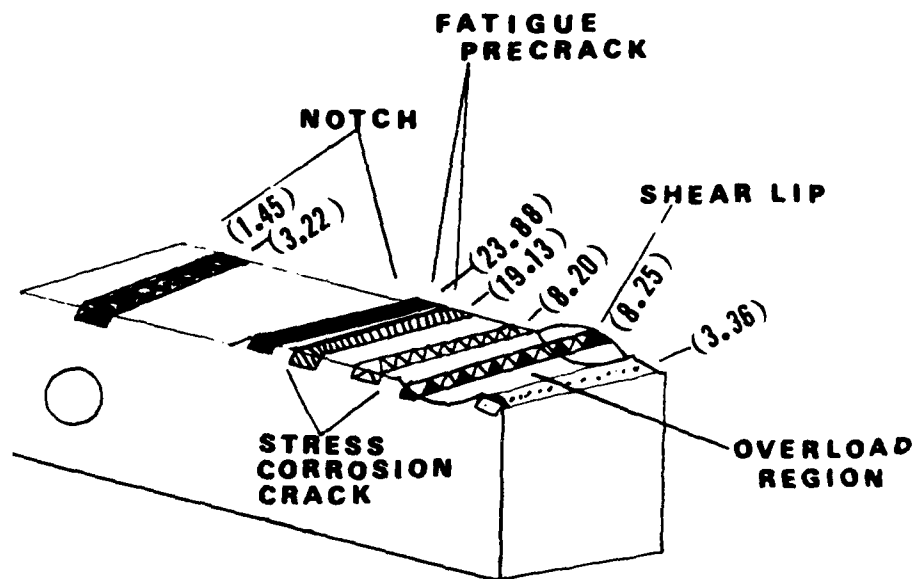


Figure 11. Localized Hydrogen Analysis - D6AC Fractured in Distilled Water and Frozen in Liquid N₂.

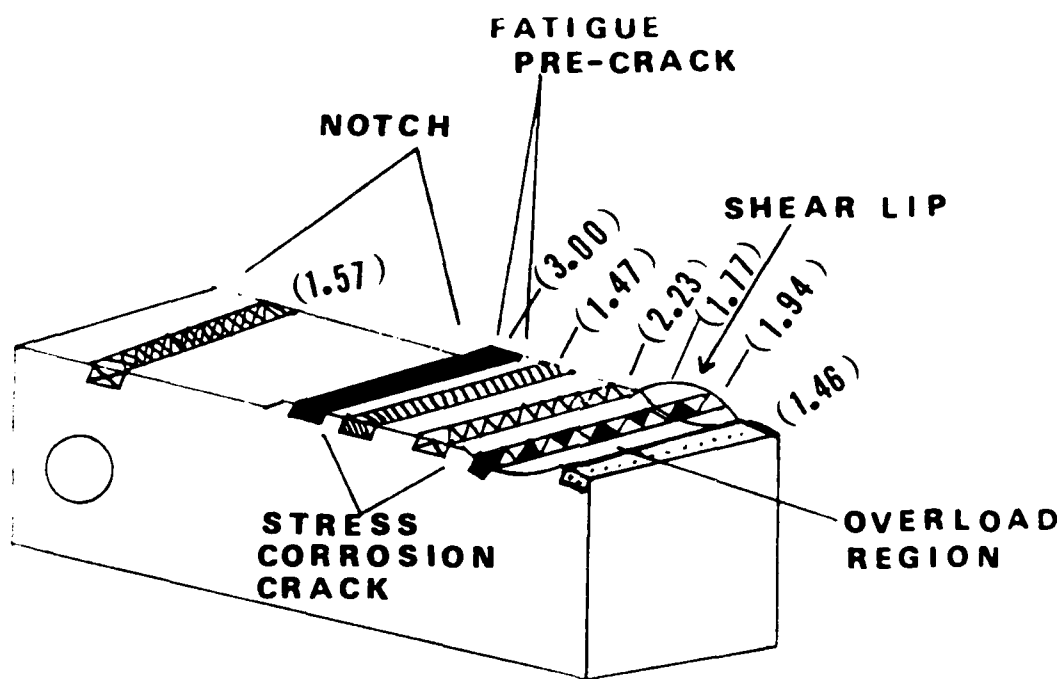


Figure 12. Localized Hydrogen Analysis, D6AC Fractured in Distilled Water Plus 2% Hydrazine and Frozen in Liquid N_2 .

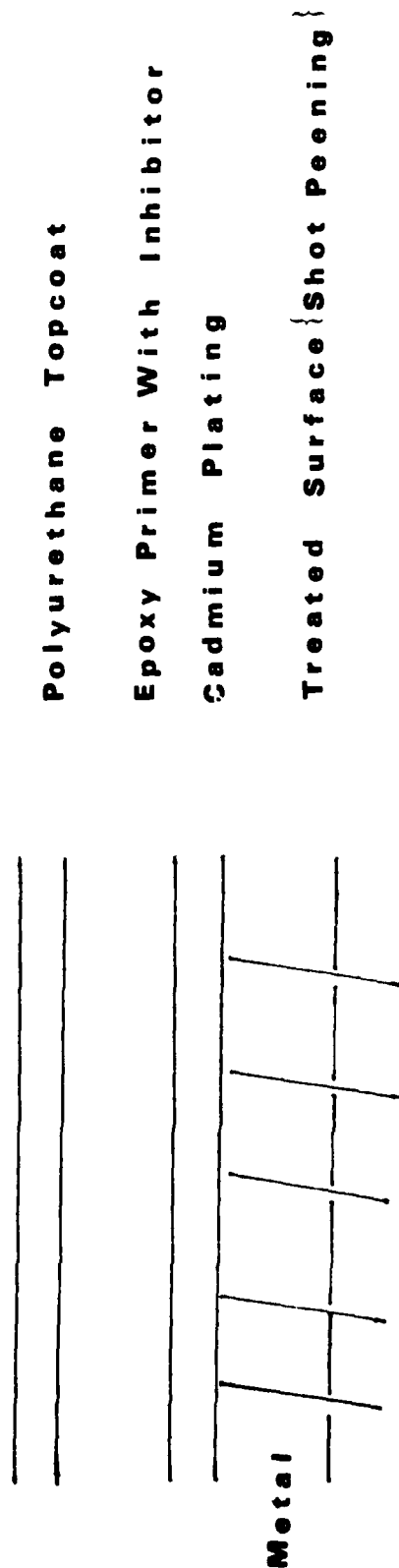


Figure 13. Environmental Protection High Strength Steel.

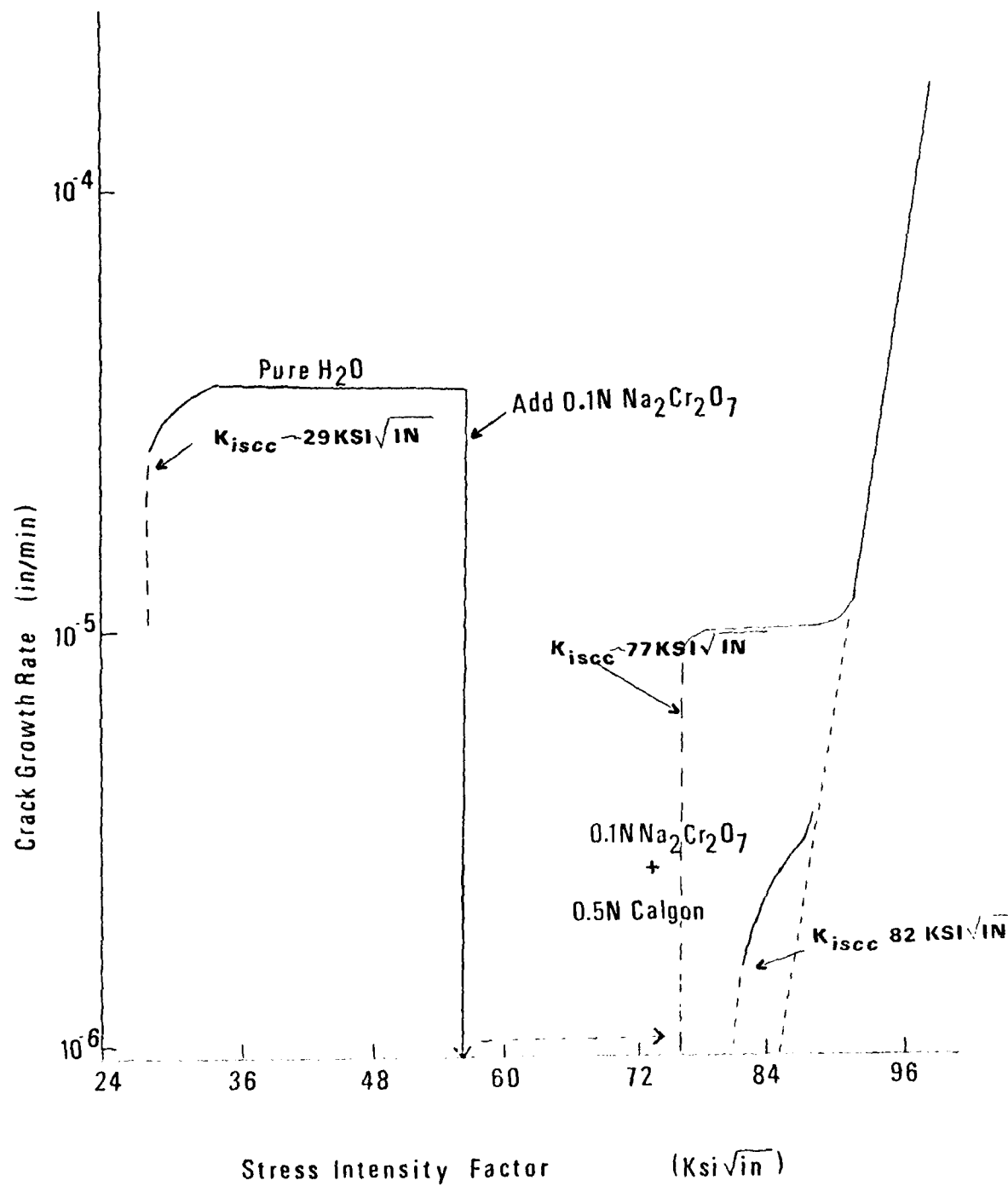


Figure 1h. Crack Growth in Distilled Water; Then Sodium Dichromate and Calgon Added

REFERENCES

1. E.H. Phelps; Proceedings of The Ohio State University Conference on Stress Corrosion Cracking, 1969.
2. B.W. Wilde, Corrosion 27, 1971.
3. B.F. Brown, Rapports Techniques, 112 RT 170 (1970).
4. T.P. Groeneveld, E.E. Fletcher and A.R. Alsea; Final Report, NASA Contract 8-20029, George C. Marshall Space Flight Center, Huntsville, AL, June 23, 1969.
5. O.M. Katz and J.A. Berger, Trans. Met.Soc. AIME, 223, 1005 (1965).
6. L.S. Darken and R.P. Smith, Corrosion 5, 1, 1949.
7. A.R. Troiano, Transactions ASM, 52, 54 (1960).
8. P.P. Cottrell, Progress in Materials Science, 9, 4, 201 (1961).
9. A.S. Tetelman; Fracture of Solids, Interscience, New York (1963).
10. K. Farrell and A.G. Quarrell, J. Iron and Steel Institute, 202, 1002 (1964).
11. E.E. Fletcher, W.E. Berry and G.A. Elsea, DMIC Report No. 232 (1966).
12. A.S. Tetelman and A.J. McEvily; Fracture of Structural Materials, Wiley, New York, 1967.
13. J. McBreen and M.A. Genshaw; Proceedings of The Ohio State University Conference on Stress Corrosion Cracking, 1969.
14. C. Zappfe and C. Sims, Trans. AIME, 145, 225 (1941).
15. F.J. deKazinsky, J. Iron and Steel Institute, 177, 85 (1954).
16. F. Garafolo, Y. Chow and R. Ambegaoka, Acta. Met., 8, 504 (1960).
17. B.A. Bilby and J. Hewitt, Acta. Met., 10, 587 (1962).
18. A.S. Tetelman and W.D. Robertson, Acta Met., 10, 775 (1962).
19. A.S. Tetelman and W.D. Robertson, Acta Met., 11, 415 (1963).
20. E.A. Steigerwald, F.W. Schaller and A.R. Troiano, Trans. Met. Soc. AIME, 215, 1048 (1959).
21. H.H. Johnson, J.G. Morlet and A.R. Troiano, Trans. AIME, 212, 526 (1958).

22. E.A. Steigerwald, F.W. Schaller and A.R. Troiano, Trans. AIME, 212, 832 (1960).
23. R.A. Oriani, Berichte de Bunsen - Gesellschaft fur physikalische Chemic. 76, 848 (1972).
24. M. Pourbaix, Corrosion Research Conference of National Association of Corrosion Engineers, Philadelphia, 1970.
25. K.D. Efird; M.S. Thesis, University of Florida, 1970.
26. P.A. Parrish, M.S. Thesis, University of Florida, 1970.
27. B.F. Brown, C.T. Fuji and E.P. Dahlberg, J. Electrochem. Soc., 116, 218 (1969).
28. J.A. Smith, M.H. Peterson and B.F. Brown, Corrosion, 26 (1970).
29. H.P. Lechkie and A.W. Loginau, Corrosion, 24, 291 (1968).
30. P.A. Parrish, C.T. Lynch, H.P. Kirkpatrick and A. Pigeaud; Proceedings of 1972 Tri-Service Conference on Corrosion, Houston, Dec. 1973.
31. P.A. Parrish, Ph.D. Thesis, University of Florida, June 1974.
32. K.B. Das; Air Force Materials Laboratory TR-73-244, Wright-Patterson AFB, OH (1973).
33. E.D. Verink, Jr. and J.M. Johnson, Annual Report, Air Force Materials Laboratory Contract F33(615)-73-C-5007.
34. E. Kuhn, Aqua Ind., 8 (41) 6 (1966).
35. C. Zanchin, Chem. Ind. (Paris) 72, 941 (1954).
36. U.R. Evans; The Corrosion and Oxidation of Metals, Arnold, London (1960).
37. W.L. Jolly; The Inorganic Chemistry of Nitrogen, p. 60, W.A. Benjamin, Inc. 1964.
38. W.M. Latimer; Oxidation Potentials, Prentice-Hall, Inc, Englewood Cliffs, NJ (1952).
39. M. Pourbaix; Atlas of Electrochemical Equilibria in Aqueous Solution, Pergamon Press, NY (1966).
40. J.I. Bregman, Corrosion Inhibitors, MacMillan Company, NY (1963).